Article
Beitr. Phys. Atmosph., February 1995, p. 59–74
0005-8173/95/01 0059–16 $ 3.00/0
Vol.68, No. 1

The Impact of El Niño- and Volcanic Forcing on the Atmospheric Energy Cycle and the Zonal Mean Atmospheric Circulation

by U. ULBRICH[1], H. -F. GRAF[2] and I. KIRCHNER[2]

[1]Institut für Geophysik und Meteorologie der Universität zu Köln, Kerpener Str. 13, 50923 Köln, Germany
[2]Max-Planck-Institut für Meteorologie, Bundesstr. 55, 20146 Hamburg, Germany

(Manuscript received May 20, 1994; accepted November 7, 1994)

Abstract

The effects on the atmospheric circulation imposed by El Niño-induced SST-forcing ("El Niño-forcing"), by volcanic dust induced stratospheric heating and reduction of solar radiation ("volcanic forcing") and by a combination of both are investigated using permanent January runs of the low-resolution (T21) ECHAM2-GCM. Considering zonally averaged quantities related to the atmospheric energy cycle, we find two features that are unique for the forcings: the Hadley circulation is increased with El Niño-forcing present, and the stratospheric jet of the winter hemisphere is increased with volcanic forcing. Combined forcing produces both anomalies simultaneously. Other anomaly structures are excited no matter which forcing is active, and it is mostly the local anomaly amplitudes that vary. Thus, the other zonal mean anomalies are not suitable for a separation of signals. One of the features common to both forcing is an increase of heat transports by stationary eddies. It causes decreased tropospheric temperatures at 30°N. It is in contrast to expectations from linear model studies that this modification of the stationary waves is associated with the opposing stratospheric wind anomalies induced by El Niño- and volcanic forcing. In accordance with the reduced temperature gradients poleward of 30°N, local contributions to baroclinic energy conversions by transient eddies are smaller than in the control run. This means that, with respect to the zonal mean temperature signal, the transient eddies are counteracting the anomaly imposed by the stationary eddies.

Zusammenfassung

Auswirkungen von El Niño-Ereignissen und Vulkanismus auf den atmosphärischen Energiezyklus und die zonal gemittelte atmosphärische Zirkulation

Anhand von Modell-Experimenten mit dem niedrig auflösenden (T21) ECHAM2-Zirkulationsmodell werden unter permanenten Januar-Bedingungen Veränderungen der atmosphärischen Zirkulation untersucht, die durch erhöhte Meeresoberflächentemperaturen während El Niño („El Niño-Antrieb"), durch vulkanisch induzierte Veränderungen der solaren Strahlung („vulkanischer Antrieb") sowie durch ein gleichzeitiges Auftreten beider Effekte hervorgerufen werden. Für die betrachteten zonal gemittelten Größen, die in Bezug zum atmosphärischen Energiezyklus stehen, werden nur zwei Effekte gefunden, die eindeutig einem Antrieb zuzuordnen sind: durch den zusätzlichen El Niño-Antrieb wird die Hadley-Zirkulation verstärkt, während durch den vulkanischen Antrieb der stratosphärische Jet der Winterhemisphäre intensiviert wird. Bei Kombination beider Antriebe werden beide Anomalien gleichzeitig angeregt. Eine Anzahl weiterer Anomalien kann durch jeden der untersuchten Antriebe hervorgerufen werden, wobei sich nur hinsichtlich der Amplituden Unterschiede ergeben. Für eine Zuordnung der Signale zu den Antrieben sind sie daher nicht geeignet. Eine der Anomalien, die durch beide Antriebe hervorgerufen werden, ist ein verstärkter troposphärischer Wärmetransport durch stationäre Wellen. Er verursacht unter anderem verringerte Temperaturen bei 30°N. Diese Modifikation der stationären Wellen geht mit gegensätzlichen stratosphärischen Windanomalien bei vulkanischem Antrieb und bei El Niño-Antrieb einher. Dies steht daher im Gegensatz zu Resultaten, die mit linearen Modellen erzielt wurden. Die Verringerung der lokalen Beiträge zu den baroklinen Energieumwandlungen nördlich von 30°N gegenüber dem Kontroll-Experiment steht in Einklang mit den örtlich verringerten meridionalen Temperaturgradienten. Die transienten Störungen wirken damit der durch die stationären Wellen verursachten Veränderung der zonalen Mitteltemperatur entgegen.

1 Introduction

One of the tasks of climatic change studies is the understanding of natural and naturally forced atmospheric variability, as this "background noise" makes an early detection of the anthropogenic greenhouse gas signal difficult. Two of the most important factors for natural variability are El Niño (see e.g. Philander (1990) and Barnett et al. (1991)) and strong, sulphur-rich volcanic eruptions (e.g. Mass and Portman, 1989; Graf et al., 1994). Even though, the determination of their influence on climate using observational data is complicated due to mainly three factors:

- Only a small period of time (compared to their typical times of recurrence) is covered by three-dimensional, high resolution observational data.
- Location, intensity (including eruption height and mass production) and chemical composition of volcanic eruptions impose variability on the forcing, as does the intensity and lateral extension of the El Niño related SST-anomalies.
- Frequently El Niño and disturbances due to volcanic aerosol occur simultaneously (Angell and Korshover, 1985; Graf 1986; Handler, 1986; Nicholls, 1986; Parker, 1988), so that for many cases only a mixed signal can be expected. Indeed, during the last decades the strong eruptions (Agung 1963; El Chichón, 1982, Pinatubo, 1991) all coincided with El Niño events.

In this paper we intend to contribute to the understanding of some of the effects of single El Niño, single volcanic and of simultaneous forcing of both factors on the zonally averaged atmospheric circulation. It is thus not attempted to speculate on possible physical or statistical reasons for the frequent coincidence. Instead, we consider the forcing effects for northern winter, using the ECHAM2 T21 atmospheric GCM. In a companion paper by Kirchner and Graf (1994, KG hereafter), horizontal anomalies produced by the same model runs are described and statistically checked. Considering temperature, wind and geopotential height fields on some pressure levels, KG find significant anomalies mainly over the tropics and the North Pacific during El Niño winters, and over the North Atlantic and parts of Eurasia during volcanically disturbed winters. In the model run with combined forcing, the anomalies are stronger than for a single forcing, but the structure of the mixed signal is very similar to that obtained with El Niño-forcing only. The model results for the combined forcing agree well with results from observational data.

In this paper, we consider zonally averaged atmospheric quantities that are related to atmospheric energy reservoirs and the energy conversion processes. This approach is chosen mainly for two reasons. First, a better understanding of the anomalies excited by the forcings by looking at changes in atmospheric processes shall be obtained. This includes the distinction of stationary and transient atmospheric waves, as the respective anomalies may come out to be either similar or opposing each other. It can also be clarified, which of both is more affected by the forcings. The second reason regards the issue of signal separation raised by KG. It shall be investigated, if zonally averaged quantities are as suitable for distinguishing the different forcing influences as horizontal distributions.
Starting with a brief description of the model and the experiments carried out, we will use the global energy cycle as the starting point for more detailed investigations of features of the zonally averaged circulation and their interrelation, emphasizing the surprising similarity of anomalies imposed by the different forcings.

2 Model and Experiments

In the present study we used the model runs described in KG. They are based on the T21 version of the ECHAM2 GCM as described by Roeckner et al. (1992), and in the DKRZ-Report No. 6 (1992). The uppermost of the 19 vertical sigma levels is at 10 hPa, and the smallest wavelength resolved by the wavenumber 21 triangular truncation is 13°. The time step is 40 minutes. This model has also been used in a recent study of the atmospheric effects of "La Niña (von Storch et al., 1994). All integrations were performed in the perpetual January mode with daily cycle over 60 Januaries for each of the four experiments (CTRL, VOLC, ENSO, VOEN). There are some differences between our perpetual January reference experiment (CTRL, with climatologically prescribed sea surface temperature and without additional aerosol forcing) and a control run of the same model version including a seasonal cycle, which are mostly due to the cooling of the Eurasian continent and warming over the Antarctic continent and the Southern Hemisphere mid-latitudes. The implications on the representation of the observed atmospheric energy cycle are comparatively small (see Section 4). Since we consider anomalies computed from different model runs which are all in perpetual January mode, we do not expect a systematic influence on our results.

The reference experiment (CTRL) is first compared to an experiment is for the El Niño case (ENSO). The atmospheric model conditions are the same as for the CTRL experiment, but the sea surface temperature anomalies in the area between 25°N and 25°S, as observed in the El Niño January 1983, were added to the mean sea surface temperature.

Since the internal radiation scheme of the ECHAM2 climate model uses a climatologically prescribed aerosol distribution, the "anomaly forcing" technique (see also Graf et al., 1993) was used to introduce volcanic forcing into the respective model runs (VOLC, VOEN). First, the volcanic aerosol effects were estimated using the combined ECHAM2 model and an external radiation-aerosol model of SCHULT (1991) based on the δ-Eddington approximation for the radiation transport equation (Bakan, 1982). The aerosol parameters were adapted from observations after the El Chichón (1982) and Pinatubo (1991) eruptions. This model was run parallel to the original ECHAM2 radiation code once with and once without the prescribed aerosol and with the atmospheric conditions from the climate model. The flux differences of the two δ-Eddington computations were then added to the results of the original code. After six months of computation, stable mean monthly anomalies of the radiative fluxes and heating rates evolved. The computed heating rates in the lower stratosphere, and the shortwave radiation effect for January conditions of the first winter after a violent tropical eruption were then used to force the climate model for all volcanic forcing experiments. Thus, in the volcano run (VOLC) the boundary conditions are the same as in the control case, but external heating rate anomalies with a maximum of 0.3 Kelvin per day are added in the stratosphere, i.e. to the upper six model levels. The shortwave radiation reduction effect was simulated with the reduction of the solar radiation at the top of the model atmosphere (about 2 W/m^2 in low latitudes and 10 W/m^2 in high latitudes). More details on this procedure are given in KG.

In the fourth experiment (VOEN) the El Niño experiment boundary conditions were combined with the heating rates and the shortwave radiation reduction corresponding to the volcano experiment.

All three forcing experiments are compared against the control experiment. A local t-test is used to estimate the statistical significance of the anomalies computed from the different 60 month means. Because of the data dependence in permanent runs, the effective number of degrees of freedom was reduced to 30 according to autocorrelation estimates by KG. Anomalies exceeding the 95 %-level of significance following this test are considered to be a stable part of the signal.

3 Observational Data

The anomalies obtained from the model runs are also compared with global ECMWF analysis data. The observed mean parameters of the non-El Niño – Januaries 1984, 1985, 1986, 1988, 1990, 1991 are compared with the mean of the El Niño – Januaries 1983, 1987 and 1992. Two of those (1983 and 1992) are combined El Niño-Volcano Januaries. It must be emphasized that, besides this inhomogenity with respect to volcano impact, the degree of insecurity associated with the observed signal is large mainly for three further reasons, namely the small number of events, systematic differences between the El Niño-events, and the impact of changes in ECMWF analysis-forecast scheme. This leads to a high variance of El Niño and non-El Niño means, so that the results from observational data are generally statistically insignificant. Even though, using this data is apparently the only way to compare the modelled anomalies to observations. In order to improve the signal strength, we compared El Niño and non-El Niño winters for analysis data, while for the model the results under El Niño boundary conditions are compared to results for climatological boundary conditions.

4 Results

4.1 The Global Energy Cycle

The results for different quantities in the global mean energy cycle are given in Table 1. The symbols denote (see Ulbrich and Speth, 1991, for the respective formulae):

- KZ – kinetic energy of the zonal mean current
- AZ – available potential energy of the zonal mean
- CZ – conversion from AZ to KZ by the mean meridional circulation
- K_{SE} – kinetic energy of the stationary eddies
- A_{SE} – available potential energy of the stationary eddies
- CA_S – baroclinic conversion from AZ to A_{SE} (due to stationary eddies)
- CE_S – baroclinic conversion from A_{SE} to K_{SE} (due to stationary eddies)

Table 1 The globally averaged energy cycle of the atmosphere for January. Mean values for non-El Niño years from ECMWF analyses (first column, see Section 3), mean values for the CTRL model run (second column), anomalies of the runs ENSO, VOEN and VOLC compared to CTRL and difference for the mean of El Niño-years 1983, 1987 and 1992 against values from column 1 (last column). Signals significant at the 5 %-level according to a t-test are shaded. Values for the energy reservoirs are given in $J/(m^2 \cdot Pa)$, for energy conversions in W/m^2.

	Analyses non El Niño	CTRL	ENSO-signal	VOEN-signal	VOLC-signal	Analyses signal
KZ	8.40	8.54	0.51	0.46	– 0.07	0.29
AZ	45.76	41.0	1.35	0.97	– 0.11	– 0.57
CZ	0.01	0.14	0.05	0.05	0.04	0.06
K_{SE}	2.63	2.30	0.08	0.27	0.30	0.02
A_{SE}	3.04	3.32	0.21	0.43	0.33	0.07
CK_S	– 0.27	– 0.33	0.05	0.01	0.00	0.11
CE_S	0.71	1.04	0.04	0.08	0.03	– 0.06
CA_S	0.88	0.95	0.07	0.13	0.09	– 0.10
K_{TE}	5.28	4.31	0.0	0.02	0.00	0.34
A_{TE}	2.87	2.87	0.05	– 0.07	– 0.07	0.17
CK_T	– 0.48	– 0.29	0.02	0.03	0.04	0.00
CE_T	1.73	1.82	– 0.01	– 0.02	– 0.03	0.10
CA_T	1.47	1.13	– 0.01	– 0.03	– 0.06	0.01

CK_S – barotropic conversion from KZ to K_{SE} (generally found to have a negative sign)

K_{TE}, A_{TE}, CA_T, CE_T, CK_T denote the same reservoirs and conversions for transient eddies.

Before we discuss the details of the anomalies due to the different forcings, we must consider how realistic the basic state of the model is compared to observations. The agreement between the global energy cycle estimated from analysis data and from the control run is fairly good. The deviations found for some of the parameters (Table 1, columns 1 and 2) are about the same as those identified by Ulbrich and Ponater (1992), who used a control run of the ECHAM2 model version that included an annual cycle. The only exception is for kinetic energy, which is about 5 % larger in the perpetual January control run used here. The origin of this latter effect is an increased intensity of the subtropical jet in the Northern Hemisphere (not shown).

The anomalies resulting from the different model forcings are shown in column 3 to 5 of Table 1, those estimated from ECMWF analysis data are given in column 6. For most parameters the changes are not statistically significant. Apparently, the variability of the different quantities is large compared to the imposed changes. Even if we disregard the lack of significance for a moment, there is no simple relation between the anomalies produced by the different forcings. It is only for some of the parameters that the anomalies for the VOEN-run are about equal to the sum of those produced by single forcing only for some parameters (e.g. KZ, CE_S, CA_S). For other parameters, this anomaly is about the average of the single forcing anomalies (e.g. CE_T, CA_T), for others it is neither of both (K_{SE}, K_{TE}).

Comparing the modelled anomalies with the estimates from analysis data, it comes out that the latter are sometimes not even within the range of values given by the different model forcings. Summing up, there is no common basis for a simple description of the anomalies imposed on the different parameters of the global energy cycle. It will become evident in the next section, that this negative result is only

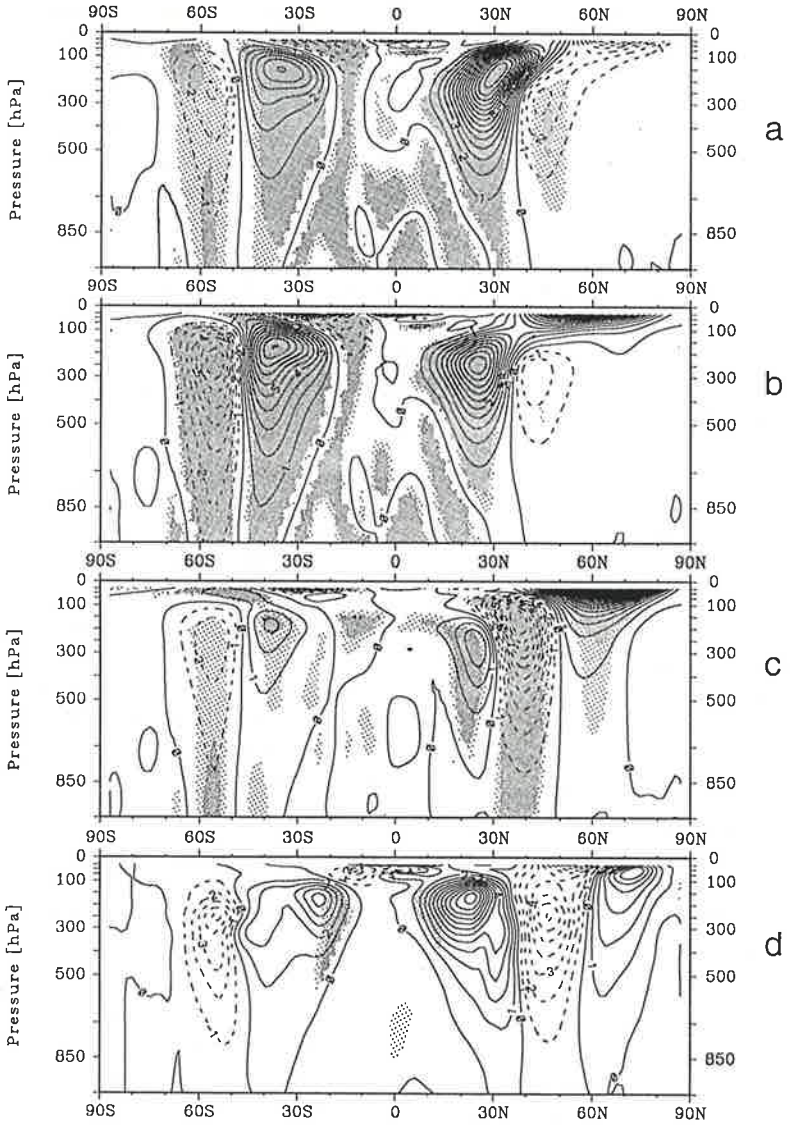

Figure 1 Signal for zonal kinetic energy (KZ) from model runs with a) El Niño forcing, b) combined forcing, c) volcano forcing, d) from ECMWF analyses. The contour interval is 1 J/(m^2 · Pa). Light/heavy shading indicates statistical significance at the 5 % /1 % level.

valid for the global values, while more can be learned from considering the related zonally averaged contributions in the following section.

4.2 Latitude-Height Distribution of Anomalies

4.2.1 Zonal Kinetic Energy

Zonal kinetic energy, KZ, is dominated by the subtropical jets of both hemispheres (Figure 1). A common structure of anomalies is found in all model experiments. The subtropical jets are intensified chiefly at their equatorial flanks, while they are somewhat weakened at their poleward flanks, which means an equatorward shift of the jet axis. Beyond this overall similarity, there are clear differences between the three anomalies. For the ENSO-run (Figure 1a) the jet intensification at the Northern Hemisphere is the dominant feature. It amounts 20 % in the jet core. For the volcano case (Figure 1c) the weakening of this jet dominates. The strongest signal for this forcing is the intensification of the polar dominates. The strongest signal for this forcing is the intensification of the polar night jet in the lower stratosphere and upper troposphere,

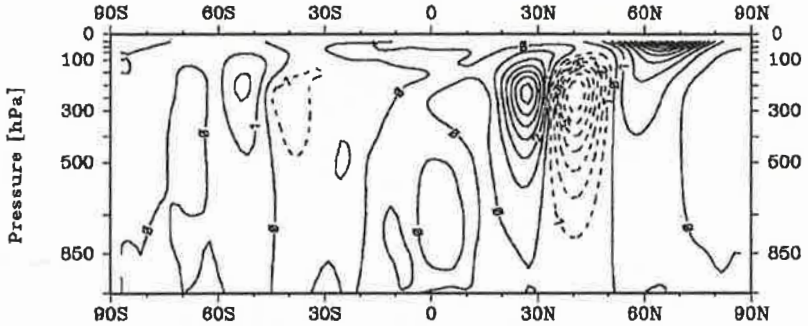

Figure 2 Difference between the sum of anomalies for El Niño- and volcano forcing and that for combined forcing, for KZ. The contour interval is 1 J/(m^2 · PA).

which is contrast to a (statistically insignificant) tendency for a weakening of this jet in the ENSO run (Figure 1a).

The combined forcing (Figure 1b) seems to produce an anomaly which is the sum of the two single forcings. This assumption of linearity can best be checked by computing the difference between the sum of single forcing anomalies and the combined forcing anomaly (Figure 2). This figure shows small values at the Southern Hemisphere, indicating that the change due to combined forcing is indeed approximately the sum of the anomalies for volcanic and El Niño-forcing. At the Northern Hemisphere, however, the structure in Figure 2 compared to that in Figure 1b suggests that the combined signal is weaker than the sum of the single forcings.

There is a general agreement of the observed anomaly (Figure 1d) and those produced by the model. Both the shift of the subtropical jets and their intensification is also found in the observational data. While neither of the model forcings is reproducing every single aspect of Figure 1d, El Niño and combined forcing are clearly closer than pure volcanic forcing. This is not unexpected since the observations are mainly (two out of three) from the mixed case.

4.2.2 Zonal Mean Temperature

It is instructive to relate the anomalies in KZ to corresponding anomalies in temperature, as a locally changed kinetic energy may be due to temperature changes in other parts of the atmosphere. The most prominent anomaly for El Niño-forcing, i.e. in the ENSO and VOEN run (Figure 3a, b), is the temperature rise in the low latitude troposphere (approx. 1 K), with maximum values at 15°S, 850 hPa and above the 300 hPa level. There is no tropospheric low latitude warming in the VOLC run. The increases in subtropical jet energies discussed in the previous section are also related to extratropical cooling. Such cooling is expected for the VOLC and the VOEN runs, as the reduced solar radiation south of about 45°N is part of imposed forcing (KG, their Figure 2). However, cooling in the subtropics appears to be a common feature of all three forcing experiments. The cold anomaly close to 30°N is similar with respect to location and amount in all three cases. It should be mentioned that this similarity of signals can hardly be detected from KG's Figure 9 because of their choice of the 850 hPa level, which is located below the level of maximal signal strength in the ENSO and VOEN runs. At the Southern Hemisphere (40°S) for the El Niño-case (Figure 3a), there is no cooling, but even in this case there is a local minimum of temperature rises.

The reduced windspeeds at the polar sides of the jets are also associated with increased temperatures at temperature and high latitudes. Again, there is a surprising similarity of all local model anomalies, though there exist some minor differences: At the Southern Hemisphere (70°S), the anomalies for the VOLC run reveal a minimum in decreasing temperatures instead of a positive anomaly (Figure 3c). At the Northern Hemisphere, the positive anomaly produced by this run is limited to a latitude belt between 40°N and 60°N, while for the other runs positive anomalies extend to the North Pole. As expected, the largest temperature increase in the VOLC run is not in the troposphere but in the stratosphere. The direct "volcanic" heating is also visible in the VOEN-run (Figure 3b), causing the increase of the Polar Night Jet's intensity visible in Figures 3b and 3c.

The observational data (Figure 3d) indicate temperature changes with a similar structure as obtained from the model runs. This regards the low latitude temperature increases, the decreases in the subtrop-

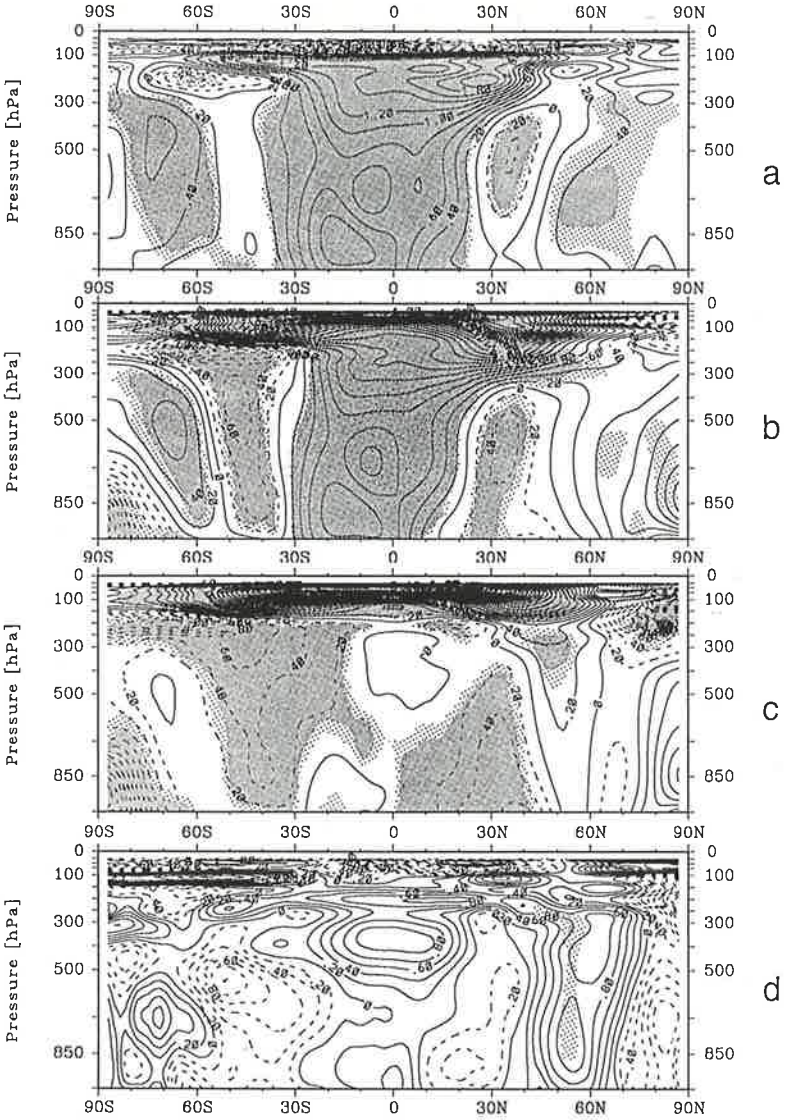

Figure 3 Signal for zonal mean temperature from model runs with a) El Niño forcing, b) combined forcing, c) volcano forcing, d) from ECMWF analyses. Contour interval: 0.2 K.

ics as well as increasing temperatures in the temperate latitudes, especially in the Northern Hemisphere. However, none of the model runs is producing all the features that appear in Figure 3d. It is a puzzling fact that there is no evidence of volcanic heating of the low latitude lower stratosphere in the observational data. We suggest that this is due to the bad quality of ECMWF analyses for the stratosphere in 1983 (Trenberth, 1992) and to the missing of volcanic forcing for January 1987. For 1992, independent observational data indicate that there was only a small temperature increase in the tropical stratosphere (Christy and Drouilhet, 1994, their Figure 4).

4.2.3 Anomalies in the Hadley Circulation

The zonal mean temperature anomalies in the tropics occurring in the ENSO and VOEN runs can largely be explained with associated changes in the Hadley circulation and the humidity field. In the runs including El Niño (and also in observations) both humidity and the upward vertical wind ($dp/dt < 0$) are increased in a 20° latitude band in the equatorial region, where the SST is locally increased (Figure 4a, b, d). Thus, more sensible and latent heat are transported upward, causing the rising temperatures in the upper tropical troposphere. For reasons of mass conservation, anomalous upward

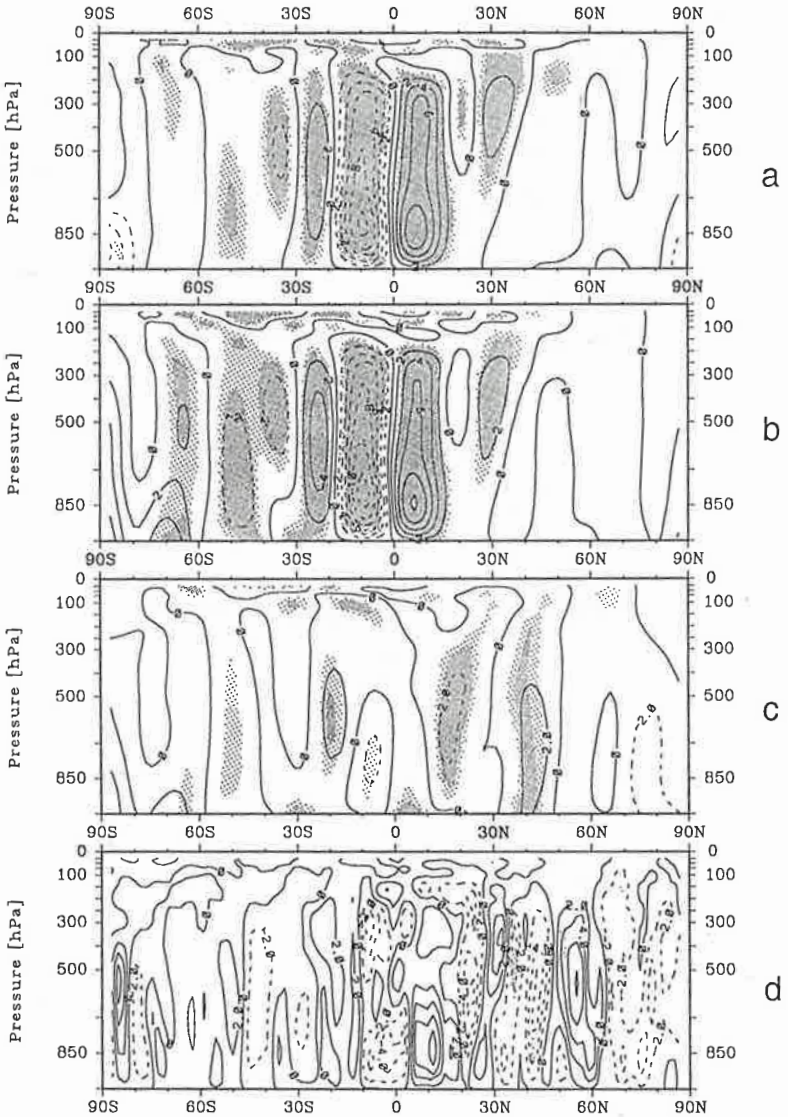

Figure 4 As Figure 1, but for the zonally averaged vertical windspeed dp/dt. Contour interval: $2 \cdot 10^{-3}$ Pa/s.

winds must be compensated by downward winds at other latitudes. Remarkably, it is only in a part of the northern branch of the Hadley cell that the sinking motion ($dp/dt > 0$) is intensified: While in the CTRL-run there is sinking motion from 5°N to 45°N, it is only intensified south of 15°N in the El Niño-forcing runs. The (much weaker) southern hemispheric branch is hardly affected by the additional forcings.

The anomalies in the mean meridional circulation affect the energy conversion CZ, which is positive when warm air is rising and cold air is sinking in the zonally averaged circulation. For the ENSO and VOEN experiments the changes of the Hadley circulation are the main cause of the global anomalies of CZ given in Table 1. In the case of only volcanic forcing (VOLC, with no large changes in the tropics, Figure 4c) the increase of the globally integrated value originates from an extratropical change of the northern branch of the Hadley cell. The structure of the anomalies at 10–50°N indicates a poleward shift of this branch, leading to a subsidence of cooler air and thus to a positive contribution to the CZ-anomaly.

4.2.4 Anomalies in the Meridional Heat Transports

The changes of the Hadley cell in the model runs with increased SST appear not to be (directly)

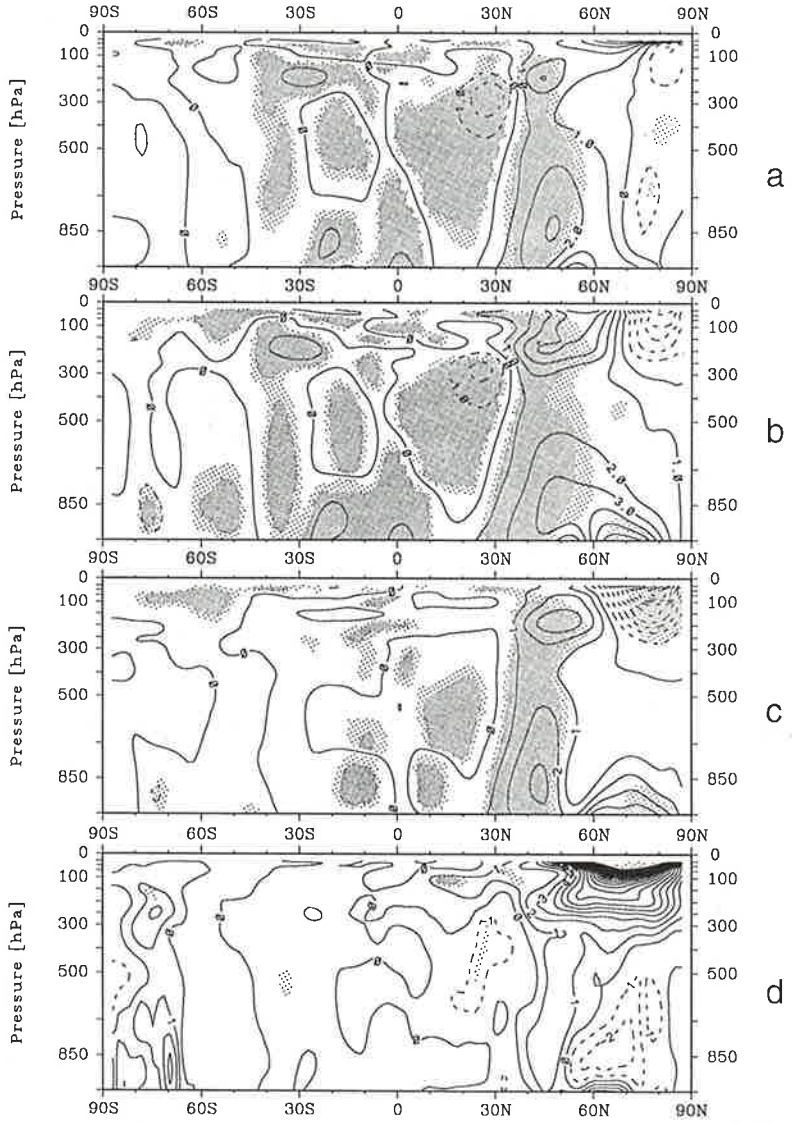

Figure 5 As Figure 3, but for the stationary eddy induced meridional heat transports, v*T*. Contour interval: 1 K m/s.

responsible for the subtropical and extratropical parts of the temperature signal. For example, Figure 4a, b indicate increased sinking at 30°N in the upper troposphere, which is fed from the Hadley cell. This gives a contribution towards a local increase of temperatures instead of the observed reduction (Figure 3a, b). The real cause for the temperature reductions in the subtropics of the Northern Hemisphere may originate from a local anomaly in the poleward transport of sensible heat due to the stationary eddies. In all three model runs, the anomalous heat-transport due to the stationary waves (Figure 5) is divergent at the region with lowered temperatures. Farther poleward (40–60°N), where this flux is convergent, the local temperatures are increased (Figure 3a, b, c). The change in meridional heat transports is associated with increased amplitudes of the stationary waves in the troposphere between about 30°N and 50°N in all three model experiments and also in observations (not shown). Neither the anomalous heat transports nor the wave amplitudes are thus simply dependent on the intensity changes of the stratospheric jet (see Figure 1a, b, c). This fact will be further considered in the discussion.

It should be noted that in all cases the local anomaly of heat transport by transient eddies is either small or has an opposite orientation. This again confirms that transient waves reduce the mid-latitude temperature gradients, but apparently the effect of the

stationary waves is stronger. Of course, this result for the Northern Hemisphere makes it difficult to explain the temperature changes at the Southern Hemisphere. They can hardly be produced by the small local anomalies in wave induced heat transports. It is suggested by KG's Figure 2 that at this hemisphere diabatic temperature forcing is the main factor influencing the local heat budget, while at the Northern Hemisphere the influence of anomalous heating anomalies appears to be weaker.

The reduced temperatures in the polar stratosphere north of 60°N in Figure 3c (VOLC-run) are a dynamical effect of reduced poleward heat transports by the stationary eddies (Figure 5c). The meridional structure of anomalous local heating by volcanic dust implies an enhanced temperature gradient only. The anomalous heating is smaller at high northern latitudes than in the subtropics (see Graf et al., 1993, their Figure 2a), but it is not imposing a temperature reduction at these pressure levels. So the enhancement of the polar night jet is not only a direct effect of the distribution of anomalous heating, but it is also increased by the stratospheric dynamics. In the real atmosphere sudden stratospheric warmings decrease the temperature contrasts. A minor warming was indeed observed in January 1992, contributing in part to the missing of such a signal in Figure 3d. The model version used does not resolve the stratosphere very well, and the results from the uppermost model layers should be considered with caution.

4.2.5 Barotropic Energy Conversions and Momentum Transports

Figure 6 shows that the dominant signal for the barotropic conversion CK_S in all model experiments and observations is an increase of positive contributions in areas poleward of the subtropical jet axis (30–40°N). The largest signal is found for pure El Niño forcing. Combined forcing gives a smaller contribution in this area, even though volcanic forcing produces a similar (but weaker) local effect. This non-linearity is consistent with the globally averaged result given in Table 1. To explain the origin of this effect, we consider the two factors mainly determining the barotropic conversion CK_S, the meridional transports of zonal momentum (by the stationary waves) and the local gradient of the zonal wind. As mentioned in Section 4.2.1, there are large changes of the subtropical jets and thus of the zonal wind gradients in all model experiments and in observations. It was evident from Figure 2 that the increase of zonal wind gradients is smaller with combined forcing than expected from the single forcing results. A corresponding effect is observed for the signal in the meridional transport of zonal momentum by the stationary eddies as the second main factor determining CK_S: Momentum transports at about 30°N, 150 hPa are increased with all forcings (not shown), but the increase found for combined forcing is smaller than the sum of single forcings, especially in the area poleward of the axis of the subtropical jet (Figure 7).

For the transient wave counterpart of this barotropic conversion, CK_T, the anomalies are much smaller than for CK_S, even though the globally integrated values are of similar size. We will not consider them in detail except for mentioning that the changes have to do with the same anomalies in the zonal mean jet and with changes in the momentum transports by the transient eddies on both hemispheres.

4.2.6 Eddy Kinetic Energy

In agreement with the global results from Table 1, all three model forcings result in local changes of kinetic energy of the transient and stationary waves, K_{TE} and K_{SE}, which are considerably different to the signal obtained from observational data. For K_{SE}, the signal obtained with volcano forcing (Figure 8c) even appears to have a structure opposite to the signal from observational data (Figure 8d), when the 5° poleward shift of the jets in the model's control run compared to observations is taken into account. El Niño-forcing in the model appears to have little effect on this energy reservoir (Figure 8a).

With respect to K_{TE} (not shown), all forcings lead to a rise of energy in the area of the southern hemispheric subtropical jet and over Antarctica (which is consistent with observational results). On the Northern Hemisphere, however, observational data indicate an increase of K_{TE} at 30–40°N and 60–80°N which is not reflected by any of the model experiments. Combined forcing even results in a reduction of this reservoir at the Northern Hemisphere, and thus is contradiction to the observational estimate.

5 Baroclinic Energy Conversions

The changes in the zonal mean temperature fields of the mid-latitudes found for the different model forcings and observations have an effect on the

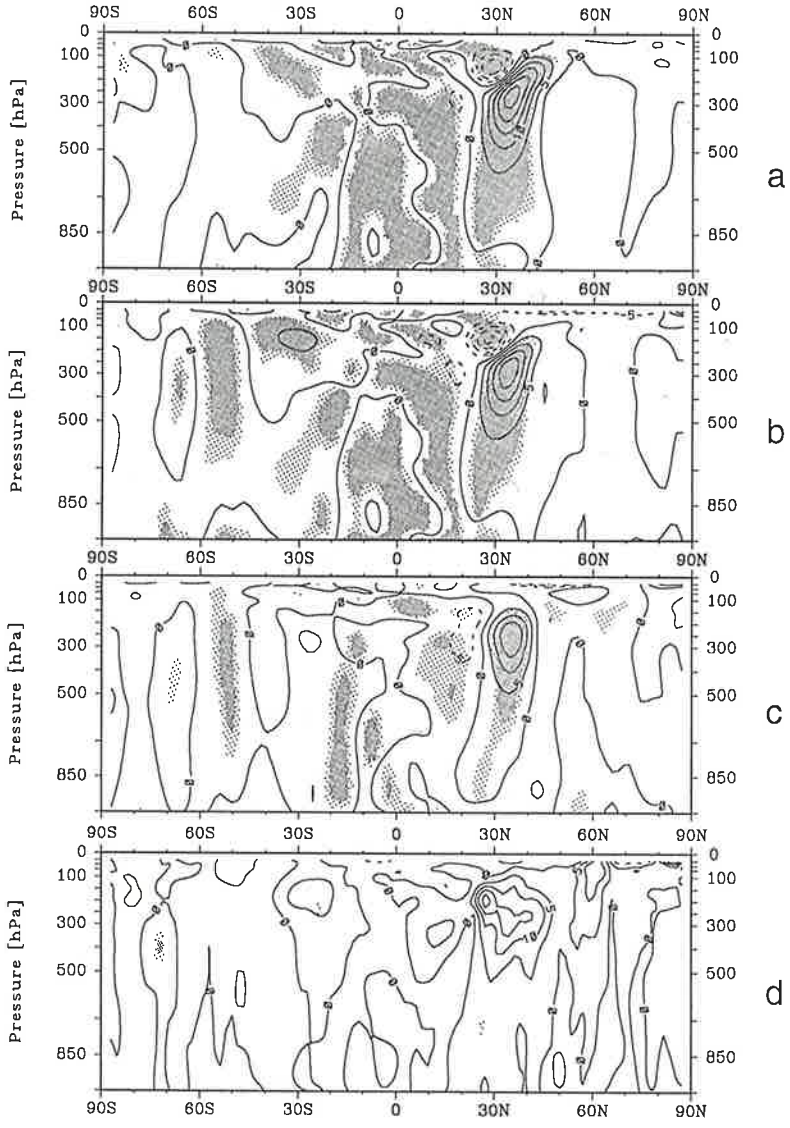

Figure 6 As Figure 3, but for the barotropic energy conversion CK_S. Contour interval: $5 \cdot 10^{-6}$ W/(m^2 · Pa).

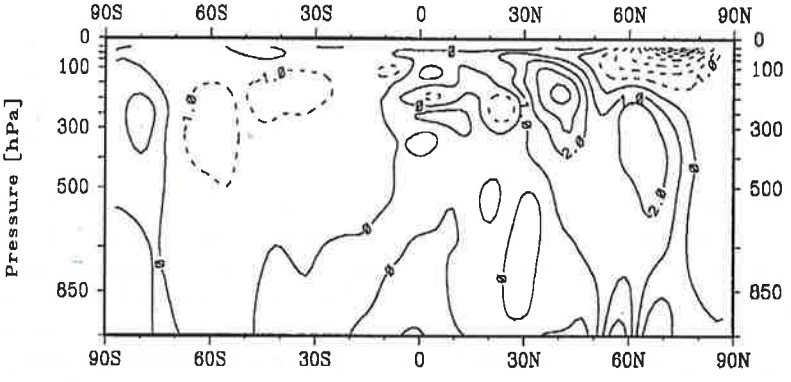

Figure 7 Difference between the sum of the El Niño plus the volcano forcing signal and the combined signal for meridional transports of zonal momentum by stationary waves. Contour interval: 1 m^2/s^2.

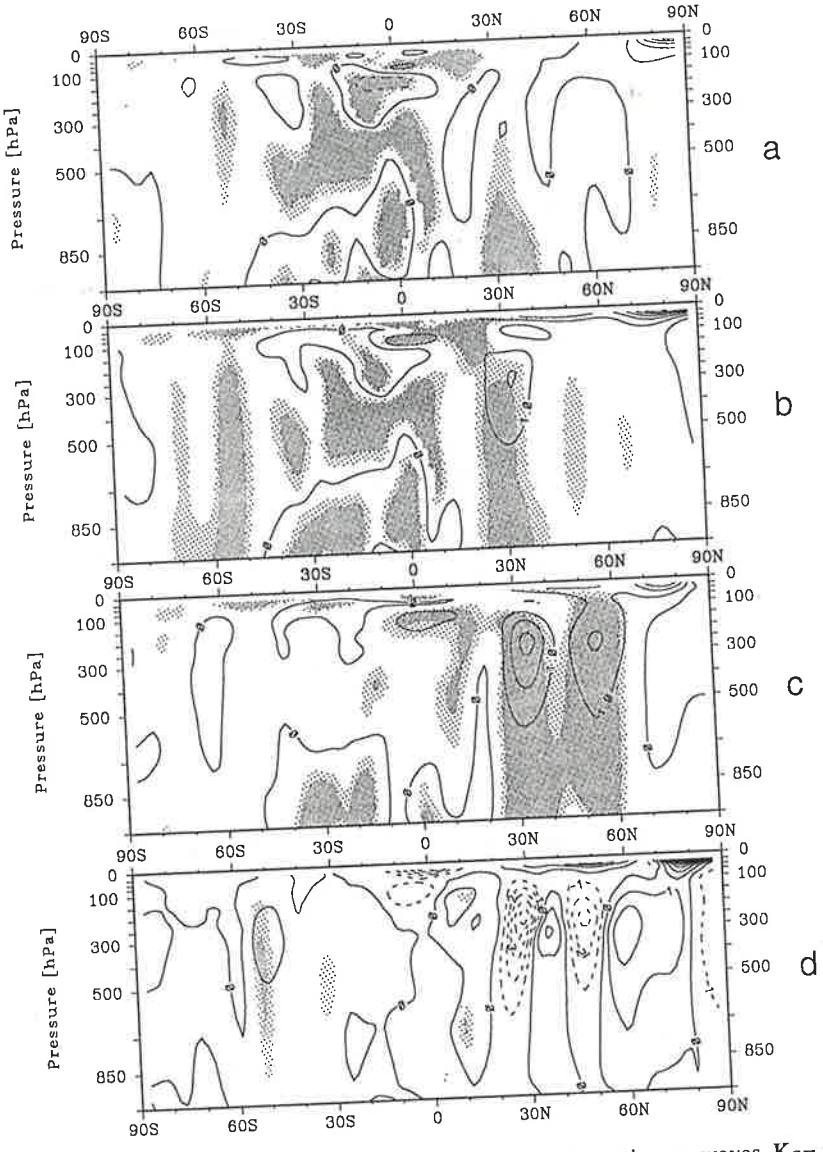

Figure 8 As Figure 1 but for the kinetic energy of the stationary waves, K_{SE}. Contour interval: 1 J/(m^2 · Pa).

meridional and vertical temperature gradient and, as a consequence, of mean baroclinicity. The local changes in baroclinic energy conversions due to transient waves (such as travelling cyclones) are expected to follow the rule that an increased temperature gradient and lowered static stability are associated with increased energy conversions and vice versa. The model anomalies in the baroclinic conversion CE_T are indeed in accordance to this rule as it can be seen comparing Figures 3 and 9a, b, c. There seems to be a contradicting effect in the observational data between 30°N and 50°N (Figure 3d): A reduced meridional temperature gradient is partly associated with locally increased contributions to the baroclinic conversion. The origin of this local anomaly is not clear, and it may well be an effect of the small sample of observational data. This suggestion is supported by the fact that in spite of the numerically large anomalies in the observational data no statistical significance is found.

Considering the baroclinic conversions due to the stationary waves, CA_S and CE_S, for the three model runs, there is a local positive anomaly at about 30°N to 50°N. It originates from the increased stationary eddy heat fluxes related to the mid-latitude temperature anomalies (see Section 4.2.4). It's signs is thus opposite to the local anomalies in the transient wave counterparts. The tendency of compensation of anomalies for stationary and transient waves is also

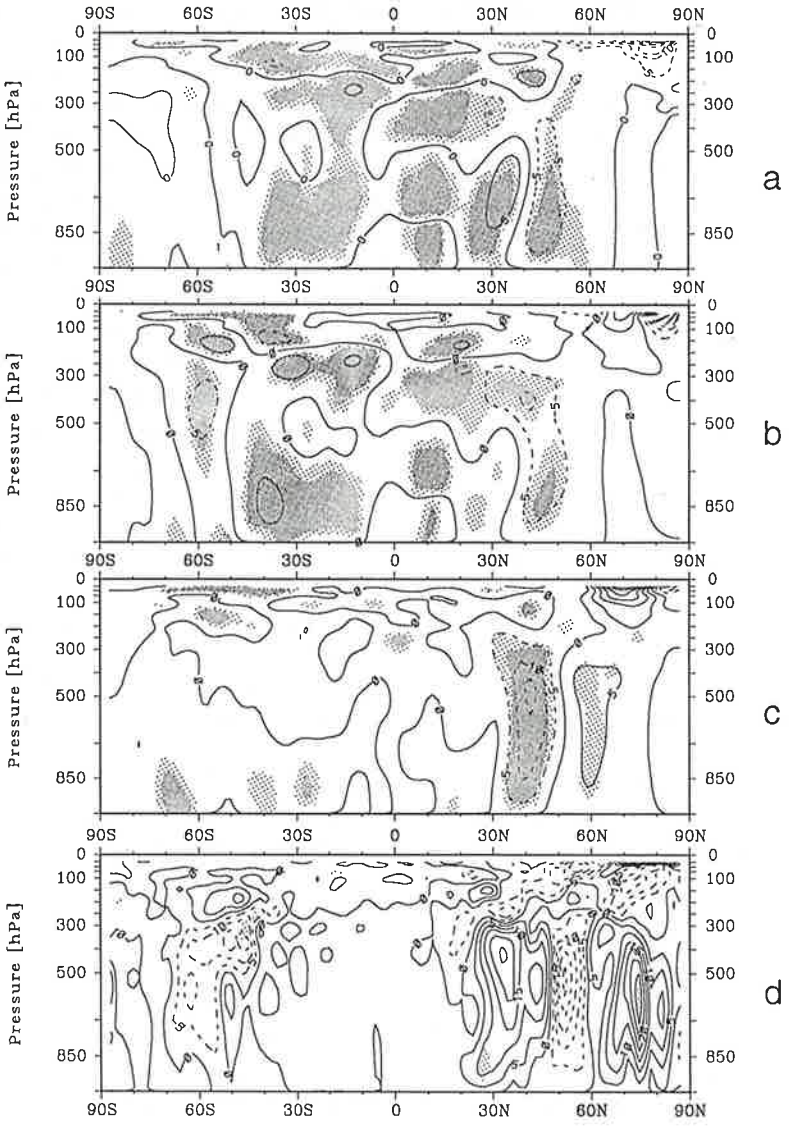

Figure 9 As Figure 3, but for the baroclinic conversion CE_T. Contour interval: $5 \cdot 10^6$ W/(m^2 · Pa).

visible in the globally averaged values given in Table 1.

6 Discussion

Using the ECHAM2-T21 GCM we have found that El Niño-forcing and volcanic forcing during northern winter produce surprisingly similar extratropical zonal mean anomalies, while stratospheric and tropical signals are different. The anomalies due to combined forcing have the structure and, at the Southern Hemisphere, also the magnitude expected from summing up the local anomalies due to single forcings. At mid-latitudes of the Northern Hemisphere the effects of combined forcing tend to be weaker than it would be anticipated from the linear sum.

Before we consider the results obtained with combined forcing we shall first relate our results for the volcanic and El Niño-forcing to other studies. The comparison shall give more insight into the physical background of the signals, besides demonstrating, that our results are not specific to the model version used.

Volcanic forcing of the atmospheric circulation has been investigated by Rind et al. (1992) and Pollack et al. (1993). Using a model with much better

resolution in the upper atmosphere than the ECHAM model used in this work, Rind et al. show that the effects of volcanic aerosol on the sea surface temperatures can be neglected for the timescale of a few years. Their results with fixed SST give about the same temperature anomalies as the VOLC experiment, i.e. cooling in the subtropical troposphere and the polar stratosphere, and warming in the tropical and subtropical stratosphere. Also the dynamical changes are about the same, including a reduction of sinking in the winter hemisphere branch of the Hadley cell at 27°N (compared to 20°N in our experiment) with weak changes (amounting 1.4 %) in its rising branch, or the increase in poleward stationary eddy transports of sensible heat around 50°N with some compensation by the transient eddies. Apparently, the effects of volcanic dust on the troposphere can be simulated without using a GCM specially designed for investigating effects in the middle atmosphere as the one used by Rind et al.

It must be stressed at this point that the anomalies induced by volcanic dust are dependent on the time scale considered. Pollack et al. (1993) reveal that volcanic dust affecting the atmosphere over a longer timescale has a different effect, with strong cooling in the whole troposphere and most of the stratosphere, and different changes to the dynamics. For the effects of a single large eruption, however, observations confirm the model results described before (Rind et al., 1992; Kodera, 1994).

The effect of increased tropical SST has been studied intensively both using simple and complex GCMs. Local positive anomalies of the tropospheric temperatures as a direct consequence of the change at the lower boundary and the equatorward shift/intensification of the subtropical jets have been reproduced using simplified two-layer quasi-geostrophic models (Wiin-Nielsen, 1986; Rao and Franchito, 1993). The structure of the temperature signal (Figure 3a) can be easily understood as an effect of the intensification of the Hadley cell due to the increased input of sensible and latent heat at the surface. It is associated with upward and poleward transport of airmasses, also including the release of latent heat in the upper levels. This mechanism appears to be linear, as "La Niña" model runs investigated by Rao and Franchito (1993) and von Storch et al. (1994) give the opposite signal, i.e. temperature reductions and poleward movement/weakening of the zonal kinetic energy in the subtropical jets.

The influence of the tropical SST-changes on the extratropical climate on the basis of zonal means has, for example, been investigated by Wu and Cubasch (1987) and Hou (1993). They also find that eddy heat transports are important for the extratropical temperature anomalies. Using a T63 high resolution version of the ECMWF model, Wu and Cubasch obtain an anomalous divergence of eddy heat fluxes between 30°N and 70°N, and anomalous convergence farther poleward. Except for the latitude where the convergence occurs (which is about 20° farther poleward), their results agree with ours: Temperatures are anomalously high in the regions of convergence, while the divergence of heat fluxes leads to reduced temperatures in lower levels of the mid-latitudes in spite of an additional heating source due to the increased Hadley circulation. According to our investigations, it is the stationary eddy induced heat fluxes which imply the temperature anomaly, while the transient eddies give an opposing contribution. A primary role of the stationary eddies for the El Niño-induced mid-latitude temperature changes is also suggested by Hou (1993). Their result was obtained considering a southern hemisphere winter case with the tropical heating anomaly placed around 15°N.

It was mentioned in Section 4.2.4 that the mechanism inducing the increased heat transports of stationary eddies in the case of El Niño-forcing is apparently not directly related to an increased stratospheric polar vortex. The increased fluxes are, however, associated with increased amplitudes of the tropospheric stationary waves in the geopotential height field. This finding is not in agreement with the mechanism KG suggested: They referred to work of Matsuno (1970) and Geller and Alpert (1980) indicating that a strong polar vortex (like it is present in the VOLC and VOEN-runs) alters the stationary wave pattern in the troposphere by reflecting vertically propagating wave energy. With the weaker than normal vortex in the ENSO run, one might expect weakened stationary waves and weakened transports by these waves, but the opposite is found. Our results can, however, still be consistent with linear theory, as Bates (1977) pointed out that there are further influencing factors on the amplitude of the geopotential height waves and the meridional heat fluxes by the stationary waves apart from the stratospheric jet intensity. Such parameters are the stratospheric wind profile, static stability, and shifts of thermal forcing structures relative to topography. A detailed study on the reasons leading to the result we obtained would require several numerical experiments with a linear model and is beyond the scope of this work.

It is interesting to note that there is some compensation of the enhanced stationary eddy heat transports by the transient eddies. This effect is apparently typical for the atmosphere, as it was reported in several observational and model studies. In case of our experiment, the physical background is obvious. The stationary eddy transports modify the meridional temperature gradient and thus the baroclinicity of the mean current. The modification of the transient wave transports can be understood as a direct consequence.

The changes in heat transports result in locally modified contributions to the baroclinic conversion rates within the energy cycle (CA_S, CA_T, CE_S, CE_T), and the same signature of anomalies is also found in their globally averaged values (Table 1). Even though not all of these conversion anomalies are statistically significant, they are clearly reflecting the signals from the subtropics of the Northern Hemisphere.

Regarding the eddy momentum fluxes and thus the barotropic conversions we found no suitable reference published for the volcanic forcing case, and so the comparison is restricted to the El Niño-forcing experiment carried out by Wu and Cubasch (1987). In contrast to our results, they obtain increased eddy momentum fluxes in the whole northern upper troposphere and stratosphere, while we find a convergence of fluxes around 45°N. Even though they used a higher resolution model, their result is less reliable, as their model version (e.g. Trenberth and Olson, 1988) is apparently not reproducing the observed time mean convergence of momentum fluxes in the mid-latitude troposphere. So it appears to be likely that the decrease in the barotropic conversions (positive sign of the anomaly) detected in this work (see Table 1) is part of the El Niño-signal.

From the similarity of single forcing anomalies it is not unexpected that combined forcing produces about the same anomaly structures as the former for many parameters and regions. The zonally averaged values are, however, mostly weaker than it would be expected from adding the anomalies for the ENSO- and VOLC runs. This is certainly important for understanding the non-linearity of the globally averaged values described in Section 4.1. Two changes can unambiguously assigned to one or the other single forcing: The intensification of the Hadley circulation with El Niño and the enhancement of the polar winter stratospheric jet with the volcanic influence. Both occur simultaneously in the combined forcing case.

The comparison of modelled anomalies with those estimated from observational data gives agreement for most parameters, even though the observed anomaly used bears a number of insecurities and inhomogeneities which, apart from the small size of the sample, lead to the missing of significance. Of course, the use of data that are heterogeneous with respect to the presence of forcings (El Niño in all cases, but not always volcanic forcing at the same time) will not prohibit the similarity of the observed and the modelled anomalies, if (as suggested by our experiments) all forcing combinations produce about the same anomaly structures for most parameters.

7 Conclusions

We investigated the effects of El Niño and strong volcanic eruptions as well as the effect of their simultaneous occurrence, using permanent January runs of the ECHAM2 low resolution atmospheric GCM. Zonal mean anomalies of basic atmospheric fields and quantities related to the energy cycle were considered.

The latitude-height distributions of the anomalies were found to have a very similar structure for most parameters, in spite of the different forcing characteristics imposed. This has important consequences for attempts to distinguish between the influences of El Niño and volcanic forcing: For the zonally averaged data, a signal separation must solely rely on the changes to the Hadley circulation and the Northern Hemispheric winter stratospheric jet. Other parameters are not suitable in this respect. In the light of KG's results, this conclusion is only valid for zonal averages, while the respective horizontal anomaly patterns may well be different for the different forcings.

It must be a consequence of the similarity of the different forcings' anomalies that the observed and modelled zonal mean anomaly structures turn out to compare well. The observational data sample we used for determining the observed anomalies is very small and heterogeneous with respect to the forcings, and thus the estimated observational anomalies turn out to be generally insignificant in a statistical sense. The agreement of modelled and observed anomalies can be taken as evidence that, in spite of the missing significance, these observational anomalies are close to the real signals.

The physical background of the observed similarities was partly explained in this diagnostic work. For example, the change in meridional heat fluxes by the stationary eddies was identified to be the cause for the temperature anomalies in the extratropical Northern Hemisphere troposphere. However, the common explanation for the stationary waves anom-

alies (see, e.g., KG) does not fit our results. The anomalies of the polar stratospheric jet's intensity were of opposite sign for El Niño and volcanic forcing, but the heat fluxes were increased in both cases. The determination of the factors leading to the same signature of heat transport anomalies in spite of the different jet anomalies using a linear model like that of Bates (1977) is left for future investigations.

Acknowledgements

We wish to thank Michael Ponater, Ulrich Cubasch, Klaus Arpe, Andreas Fink and Martin Sogalla for their comments on an earlier version of the manuscript. This study was supported by the Bundesministerium für Forschung und Technologie under grants 07KFT012 and 07KFT55A7 within the climate research program.

References

Angell, J. K. and *J. Korshover,* 1985: Surface temperature changes following the six major volcanic episodes between 1780 and 1980. J. Clim. Appl. Meteorol. **24,** 937–951.

Bakan, S., 1982: Strahlungsgetriebene Zellularkonvektion in Schichtwolken. Dissertation, Universität Hamburg, 99 pp.

Barnett, T. P., M. Latif, E. Kirk and *E. Roeckner,* 1991: On ENSO physics. J. Climate **4,** 487–515.

Bates, J. R., 1977: Dynamics of the stationary ultra-long waves in middle latitudes. Quart. J. R. Met. Soc. **103,** 397–430.

Christy, J. R. and *S. J. Drouilhet,* 1994: Variability in daily, zonal mean lower stratospheric temperatures. J. Climate **7,** 106–120.

DKRZ, 1992: The ECHAM3 atmospheric general circulation model. Technical report **6,** 184 pp.

Geller, M. A. and *J. C. Alpert,* 1980: Planetary wave coupling between the troposphere and the middle atmosphere as a possible sun-weather mechanism. J. Atmos. Sci. **37,** 1197–1215.

Graf, H. F., 1986: Abkühlung der Nordhemisphäre – ein möglicher Trigger für El Niño/Southern Oscillation-Episoden. Naturwissenschaften **73,** 258–263.

Graf, H. F., I. Kirchner, A. Robock and *I. Schult,* 1993: Pinatubo eruption winter climate effects: Model versus observations. Climate Dynamics **9,** 81–93.

Graf, H. F., J. Perlwitz and *I. Kirchner,* 1994: Northern Hemisphere tropospheric mid-latitude circulation after violent volcanic eruptions. Beitr. Phys. Atmosph. **67,** 3–13.

Handler, P., 1986: Possible association between the climatic effects of stratospheric aerosols and sea surface temperatures in the eastern tropical pacific ocean. Journal of Climatology **6,** 31–41.

Hou, A. J., 1993: The influence of tropical heating displacements on the extratropical climate. J. Atmos. Sci. **50,** 3553–3570.

Kodera, K., 1994: Influence of volcanic eruptions on the troposphere through stratospheric dynamical processes in the northern hemisphere winter. J. Geophys. Res. **99D,** 1273–1282.

Kirchner, I. and *H.-F. Graf,* 1994. Volcanos and El Niño – Signal separation in winter. Accepted for publication in Climate Dynamics (also Max-Planck-Institut für Meteorologie, Report 121, 57 pp.).

Mass, C. F. and *D. A. Portman,* 1989: Major volcanic eruptions and climate, a critical evaluation. J. Climate **2,** 566–593.

Matsuno, T., 1970: Vertical propagation of stationary waves in the winter northern hemisphere. J. Atmos. Sci. **27,** 871–883.

Nicholls, N., 1988: Low latitude volcanic eruptions and the El Niño – Southern Oscillation. Journal of Climatology **8,** 91–95.

Parker, D. E., 1988: Stratospheric aerosols and sea-surface temperatures. Journal of Climatology **8,** 87–90.

Pollack, J. B., D. Rind, A. Lacis, J. E. Hansen, M. Sato and *R. Ruedy,* 1993: GCM simulations of volcanic forcing: Part I: Climate changes induced by steady-state perturbations. J. Climate **6,** 1719–1742.

Philander, S. G., 1990: El Niño, La Niña, and the Southern Oscillation. International Geophys. Series 46, Academic Press, San Diego, 289 pp.

Rao, V. B. and *S. H. Franchito,* 1993: The response of a simple climate model to the sea surface temperature anomalies. Annales Geophysicae **11,** 846–856.

Rind, D., N. K. Balchandran and *R. Suozzo,* 1992: Climate Change and the middle atmosphere. Part II: The impact of volcanic aerosols. J. Climate **5,** 189–208.

Roeckner, E., K. Arpe, L. Bengtsson, S. Brinkop, L. Dümenil, M. Esch, E. Kirk, F. Lunkeit, M. Ponater, B. Rockel, R. Sausen, U. Schlese, S. Schubert and *M. Windelband,* 1992: Simulation of the present-day climate with the ECHAM model: Impact of model physics and resolution. Report No. **93,** Met. Inst. Univ. Hamburg, 172 pp.

Trenberth, K. E., 1992: Global analyses from ECMWF and atlas of 1000 to 10 mb circulation statistics. NCAR technical note, NCAR/TN-373+STR, 191 pp.

Trenberth, K. E. and *J. G. Olson,* 1988: ECMWF Global Analyses 1979–1986, Circulation statistics and data evaluation. NCAR technical note, NCAR/TN-300+STR, 94 pp.

Ulbrich, U. and *P. Speth,* 1991: The global energy cycle of stationary and transient atmospheric waves: Results from ECMWF analyses. Meteorol. Atmos. Phys. **45,** 125–138.

Ulbrich, U. and *M. Ponater,* 1992: Energy cycle diagnosis of two versions of a low resolution GCM. Meteorol. Atmos. Phys. **50,** 197–210.

von Storch, H., D. Schriever, K. Arpe, G. W. Branstator, R. Legnani and *U. Ulbrich,* 1994: Numerical experiments on the atmospheric response to cold equatorial pacific conditions (La Niña) during northern summer. The Atmosphere – Ocean System **1.** In press.

Wiin-Nielsen, A., 1986: On simple estimates of the impact of heating anomalies on the zonal atmospheric circulation. Annales Geophysicae **4B,** 365–376.

Wu, G. and *U. Cubasch,* 1987: The impact of El Niño anomaly on mean meridional circulation and transfer properties of the atmosphere. Scientia Sinica **30,** 533–545.